IEEE Access
Multidisciplinary | Rapid Review | Open Access Journal

Received December 29, 2020, accepted January 22, 2021, date of publication February 3, 2021, date of current version February 12, 2021.

Digital Object Identifier 10.1109/ACCESS.2021.3056456

Performance Comparison of Power Divider and Fiber Splitter in the Fiber-Based Frequency Transmission System of Solar Radio Observation

YUQING LIU[1], DAOPENG REN[1], FABAO YAN[1,2], ZHAO WU[1], ZHEN DONG[2], AND YAO CHEN[1]

[1]Laboratory for ElectromAgnetic Detection (LEAD), Institute of Space Sciences, Shandong University, Weihai 264209, China
[2]School of Mechanical, Electrical & Information Engineering, Shandong University, Weihai 264209, China

Corresponding author: Fabao Yan (hjc-8555@sdu.edu.cn)

This work was supported in part by the National Natural Science Foundation of China under Grant 41904158, Grant 11703017, and Grant 41774180, in part by the China Postdoctoral Science Foundation under Grant 2019M652385, in part by the Shandong Postdoctoral Innovation Project under Grant 202002004, and in part by the Young Scholars Program of Shandong University, Weihai, under Grant 20820201005.

ABSTRACT Time-frequency synchronization plays an important role in the construction of solar radio telescopes (such as heliograph and interferometry). In the development of a synchronization system, time-frequency signal is divided and transmitted to each antenna in an array, therefore, the performance of the signal splitting devices determines the quantity of the data. To address this situation, we designed a frequency transmitting system, and conducted a test to compare the phase difference among outputs (10 MHz - 1.4 GHz), and the deterioration of the frequency stability (10 MHz – 1GHz) brought by different splitting devices (fiber splitter and power divider). The following results had been obtained: 1) Phase difference introduced by both fiber splitter and power divider can be restricted in a range of $\pm 4°$, and the fiber splitter is rather stable, which indicate that a better imaging effect of heliograph can be achieved when using fiber splitters. 2) Frequency stability deterioration get better (worse) with increasing temperature for fiber splitter (power divider) in the testing frequency range for a short-time sampling (100 ms), and for a long-time sampling (10 min), the frequency stability of different devices is determined by both temperature and signal frequency. By estimating the SNR, the performance of optical splitter is found to be slightly better than power splitter. This article provides a basis for the selection and compensation of frequency transfer system components for integrated aperture heliograph, and provide a feasible solution of the construction of low-cost radioheliograph.

INDEX TERMS Synthetic aperture heliograph, fiber-based time and frequency synchronization, power divider, fiber splitter.

I. INTRODUCTION

During solar bursts, large amount of thermal and non-thermal particles and radiation in the entire frequency bands (e.g. radio, X-ray, gamma-ray etc.) are ejected into the inter-planetary space, which impact the solar-terrestrial environments greatly and lead to severe space weather events, such as solar energetic particle events (SEPs), magnetic storms, etc [1]–[5]. Therefore, the study of the solar activities is important in the forecasting of the space weather. Right now, white-light and radio are the two main observing windows for ground-based solar observations. In particular, the radio observation is freedom of the climate changes and has huge advantages.

The usually used solar radio instruments are solar radio flux telescope, spectrometers and radioheliograph, among which the radioheliograph, an integrated aperture radio telescope, can observe the spatial-resolved Sun. The basic unit of a solar radioheliograph is the two-element radio Interferometers, in which two antennas at certain direction and a distance interfere the received signals of the Sun to generate the visibility, i.e. the value of one point in the U-V

The associate editor coordinating the review of this manuscript and approving it for publication was Muguang Wang.

coverage [6]. Telescope arrays of different types, such as T-shape, cross-shape, spiral-shape etc., provide different combinations of baselines and yield the U-V sampling coverage of the Sun. According to the image reconstruction, we can finally get the information of the location and intensity of radiation source (the image of the Sun).

Time-frequency synchronization is one of the essential technologies in the design of a synthetic aperture heliograph [7]. Data of each antenna with timestamp is collected for the subsequent signal processing. Two signals with the same timestamp are correlated with each other, and the synchronization then determines the alignment of different signals and therefore the quality of the final reconstructed imaging of the Sun. To better align signal from different antennas, a high-precision time synchronization is needed. Meanwhile, frequency jitter will affect the signal-to-noise ratio (SNR), thus affect the measurement accuracy of the receiver [8]–[11]. Therefore, a time synchronization system with high precision which can guarantee a higher sampling accuracy is demanded.

In the constructions of the previous radioheliographs, solar radio signals are usually first modulated by optical transmitters, and then transmitted to the control room via optical fibers. Time-frequency synchronization is then carried out in the central control room where a local oscillator distributes the synchronization signal to each receiver. This kind of time-frequency synchronization has been used in the Nobeyama Radioheliograph (NoRH) [12], the Siberian Solar Radio Telescope (SSRT) [13], etc. In other cases, The Atacama Large Millimeter/submillimeter Array (ALMA) and Square Kilometer Array (SKA) distribute the synchronization signal to the receivers that mounted behind each antenna [14]–[17], however, they are not solar-dedicated. We note that in the development of the high-frequency (tens of GHz) solar radio telescopes, the phase difference and frequency stability among signals from the antennas are important influence factors in the processing of aperture synthesis. Therefore, the fiber-based timing schemes that has been used in ALMA and SKA could be a suitable option for the construction of the new-generation solar interference array [18].

There are mainly two kinds of fiber-based time-frequency synchronization using Wavelength Division Multiplexing (WDM) technology, i.e. the Round-Trip and the Two-Way method. In the Round-Trip method (see Figure 1), a time signal generated by the central clock is divided and sent to different channels (users) where each divided signal is separated into two parts. One of the separated signals at the users' end could be used as the sampling signal, and the other signal returns to the central clock to determine the time delay in the transmission [18]. According to the time difference of the two channels, the synchronization can then be achieved by using delay lines. In the Two-Way comparison method, two clocks at different ends send signals to each other through the same fiber. The time difference can be yield by comparing the

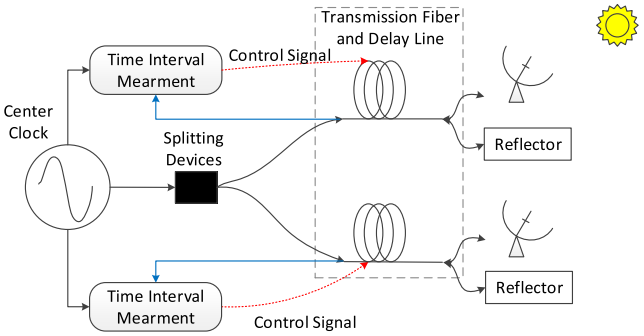

FIGURE 1. Schematic diagram of time-frequency synchronization system of the radioheliograph.

local time and the received time, and the time could then be aligned by changing one of the clocks.

We adopt the Round-Trip method to achieve time-frequency synchronization among different channels. The time delay (Δt_1 for the upper channel and Δt_2 for the bottom channel in Figure 1) could be obtained by measuring the rising edge (zero-crossing point) of the signal returned from each channel. And the time difference between the two channels is then derived as $(\Delta t_1 - \Delta t_2)/2$.

In the past, many authors have developed several methods to solve the time delay and frequency stability in the time-frequency synchronization system. For example, Liu *et al.* [19] used a cascaded fiber line to transfer the frequency and one pulse-per-second (1PPS) time signal simultaneously, Wang *et al.* [20] adopted femtosecond laser as light sources in a time-frequency synchronization system, and Zhu *et al.* [21] developed new phase noise compensation methods placed at the client site instead of the sending side. So far, the fiber splitter and power divider are usually used as the key devices of the signal splitting in a fiber-based time and frequency synchronization system, and the choice of them depends on the location of the splitter [17], [21]–[23]. These signal splitters may influence the time delay and frequency stability, and therefore impact the operation of the heliograph. However, no tests have been conducted to investigate the performance of them, and thus no relevant evaluation of the performance has been applied in the construction of the heliograph.

To realize time and frequency synchronization, we conduct tests to compare the performance of the fiber splitter and power divider as the signal splitting devices in this work. We first carried out a test to compare the phase difference introduced by fiber splitters and power dividers, and then tested the frequency stability's degradation caused by them. The next section presents the diagrams of the tests. Section 3 shows the test results. The summary and discussion are given in the last section.

II. METHODS

According to the Round-trip method, we split the time signal into two channels, and tests of the phase difference and frequency stability are then carried out.

A. PHASE DIFFERENCE

The diagrams of the phase imbalance tests for the power dividers and the fiber splitters are shown in Figure 2 and Figure 3, respectively. We note that the optical signals are transmitted by optical fibers (shown as the red lines), and the coaxial cables are used in other parts in the diagram.

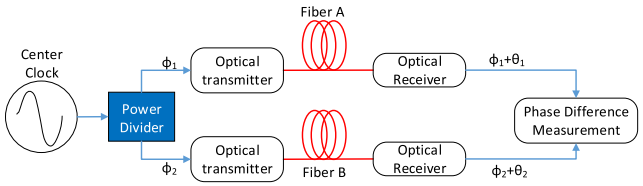

FIGURE 2. Test scheme of phase difference of power divider.

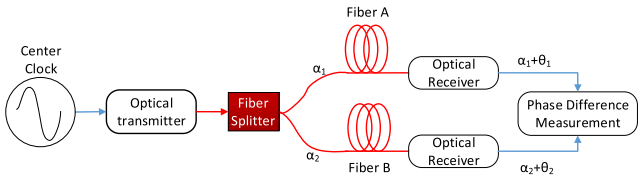

FIGURE 3. Test scheme of phase difference of fiber splitter.

As seen from Figure 2, the power divider splits the signal from the central clock into two channels and the initial phase of the two signals are φ_1 and φ_2, respectively. The two signals are then converted to optical signals by the optical transmitter and transmitted through 1-meter fibers (fiber A and B) to the optical receivers. The optical receiving module converts these signals into electrical ones with phases of $\varphi_1 + \theta_1$ and $\varphi_2 + \theta_2$ respectively, in which $\theta 1$ and θ_2 are the changes of phase introduced by devices, i. e. optical fibers, coaxial cables and optical transmitters, in each channel. Therefore, the phase difference between the two channels is $(\varphi_1 + \theta_1) - (\varphi_2 + \theta_2)$. We note that the phase difference introduced by each channel can be eliminated by exchanging devices of the two channels.

In the test for the fiber splitters (as shown in Figure 3), the time signal from the central clock should first be converted to an optical one by the optical transmitter. The fiber splitter then divides this optical signal into two channels, and the following testing diagram is the same as that used in Figure 2. The phase difference between the two channels is $\alpha_1 - \alpha_2$.

B. FREQUENCY STABILITY

Frequency stability is usually defined as the change of average frequency of the output signal during the sampling. And it can be used to assess the fluctuations of the output signal. The frequency stability could be described in both time and frequency domain. In the time domain, the frequency stability can be measured by the Allan variance:

$$\sigma_y^2(\tau) = 1/[2(M-1)] \sum_{i=1}^{M-1} (y_{i+1} - y_i)^2, \qquad (1)$$

where τ is the duration of sampling, M is the times of sampling, and y is the average frequency during the sampling interval. In the frequency domain, frequency stability is usually measured by phase noise. We use the Allan variance (in time domain) to characterize frequency stability in this article for convenience.

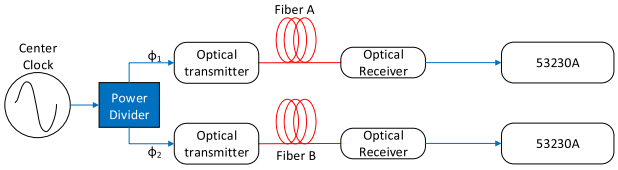

FIGURE 4. Test scheme of frequency stability of power divider.

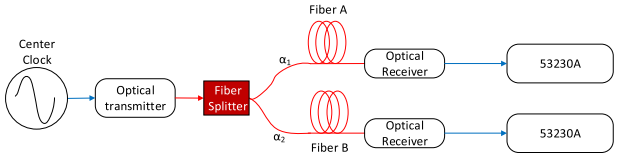

FIGURE 5. Test scheme of frequency stability of fiber splitter.

Figure 4 and Figure 5 present the testing diagrams of frequency stability for the power divider and fiber splitter, respectively. The testing configuration in Figure 4 (Figure 5) is the same as that in Figure 2 (Figure 3), except the final module, where the frequency counter 53230A is used to yield the Allan variance.

Both long-term (10 min) and short-term (100 ms) tests of the frequency stability are carried out in this work, as the long-term testing of the frequency stability usually features the stability of the frequency source, while the short-term testing can characterize the influence from the circumstance.

III. RESULTS

A. PHASE DIFFERENCE

In our test, the analog signal generator N5183B (Keysight) is used as the center clock which can generate signals in a frequency range of 9 kHz – 40 GHz. The optical transmitter F-tone FTRFT-0PN55SF-U000, and optical receiver F-tone FR-0PGB00FS-U000 are used for the conversion of electric and optical signals. The G652 fibers are used for the transmission of optical signal. To exclude the accidental error caused by devices, three power dividers (power divider 1: BayPSC-2-10; power divider 2: Mini-Clrcuits ZFRSC-2050+; power divider 3: Marki PD0R510) and three fiber splitters (fiber splitter 1 and fiber splitter 2: Fused Bi-conical Tap (FBT); fiber splitter 3: Planar Light wave Circuit (PLC)) are used in the tests. The tests are performed at a constant temperature of 25°C in a frequency range of 10 MHz – 1.4 GHz.

Figure 6 presents the phase difference between the two channels introduced by the three power dividers (see Figure 2 for the testing diagram) with changing frequency. The wavelength and power of the tested signal are 1550 nm and −5 dBm, respectively. Because of the working frequency

range of 500 MHz ∼ 10 GHz, phase difference for power divider 3 below 500 MHz is left for blank. The phase differences of power divider 1 (blue in Figure 6) and power divider 3 (black in Figure 6) fluctuate around zero, with an error of ∼ ±1°, while the fluctuation of power divider 2 (orange in Figure 6) can reach up to about 3°. We note that there is no significant dependence of the phase difference on the increasing frequency.

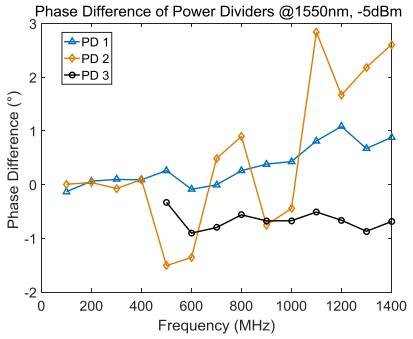

FIGURE 6. The phase difference (10 MHz - 1.4 GHz) between the two channels (shown in Figure 2) introduced by three power dividers. The wavelength and power of the tested optical signal are 1550nm and −5dBm, respectively.

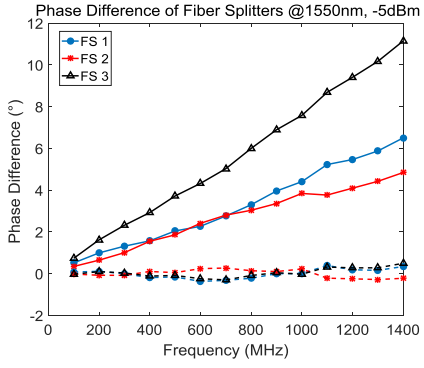

FIGURE 7. The phase difference (10 MHz - 1.4 GHz) between the two channels (shown in Figure 2) introduced by three fiber splitters. The wavelength and power of the tested optical signal are 1550nm and −5dBm, respectively.

The tested phase differences of the three fiber splitters are shown in Figure 7. The solid lines illustrate the change of phase difference between the two channels (see Figure 3 for the testing diagram) with changing frequency. We can see that the phase differences generated by fiber splitters increase with the increasing frequency approximately quasi-linearly. We assume that for a specific frequency f, the phase difference ϕ between the two channels is given by:

$$\phi = 360° \cdot f \cdot t, \tag{2}$$

where t is the time difference between the two channels (achieving an identical phase state). We can see that the phase difference can be proportional to the frequency when t is fixed. Taking the test for fiber splitter 1 (blue solid curve in Figure 7) for example, the time difference of the two channels can be yield to be about 0.014 ns. The length difference of the fibers at the rear end (after splitting signals) of fiber splitter 1 is 3 mm, which leads to a time difference of 0.015 ns according to the light speed of $\sim 2*10^8$ m/s in the fiber. Similarly, the length difference between the two fibers of fiber splitter 2 (red curves in Figure 7) is about 2 mm with a calculated time difference of 0.010 ns and the measured time difference is 0.012 ns. The length difference of fiber splitter 3 is ∼3.5 mm which lead to a time difference of 0.0175 ns, and this is also roughly consistent with the tested time difference of 0.019 ns. We can find that the measured times difference of the two channels are approximately equal to those introduced by the length difference of the fibers at the rear of the splitters. We then exclude the influence of the fiber and the corresponding results are shown as the dashed lines in Figure 7. It can be seen that the phase difference fluctuates within the range of ∼ ±1° in the entire testing frequency range. According to the above analysis, the time/frequency difference introduced by fiber splitters is mainly caused by length difference of the fibers at the rear end. The influence brought by the splitters themselves can be restricted in a phase range of ±1°.

We then deduct tests for the above splitting devices at 1310 nm, and the optical transmitter is thereby changed to F-tone FTRFT-0PN31SF-U000. The results of power dividers and fiber splitters are shown in Figure 8 and 9, respectively. We can see that similar to those in Figure 6, there is no significant dependence of the phase difference on frequency for power dividers. And results in Figure 9 also indicate that phase difference can be eliminated to a large extent when excluding the influence of the fiber at the rear end of the splitters.

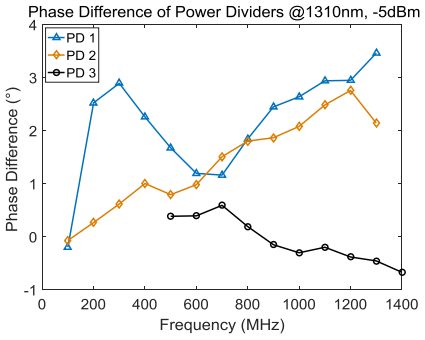

FIGURE 8. The phase difference between the two channels (shown in Figure 2) introduced by three power dividers. The wavelength and power of the tested optical signal are 1310nm and −5dBm, respectively.

When comparing the results of signal with the wavelength of 1310 nm and 1550 nm, we can find that the result for 1310 nm optical signal has a larger phase difference than that for the 1550 nm signal. We believe that this situation is mainly caused by material dispersion, with a small contribution from waveguide dispersion. As according to the dispersion characteristic of G652 fiber, the velocity of 1310 nm signal is slower than that of 1550 nm. Therefore, the transmitting time

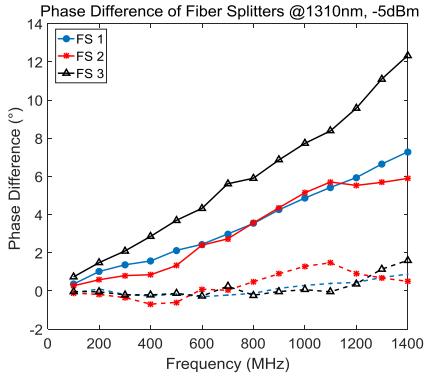

FIGURE 9. The phase difference (10 MHz - 1.4 GHz) between the two channels (shown in Figure 2) introduced by three fiber splitters. The wavelength and power of the tested optical signal are 1310nm and −5dBm, respectively.

and phase difference would be larger for 1310 nm signal. When subtract the phase difference caused by the fiber length difference, the effect of dispersion is not significant.

We further carry out tests for signals with various optical power (at 1310 nm), and the corresponding results are illustrated in Table 1. We can see that although the variation of phase difference with changing input power varies, the fluctuations are rather small and irregular. And comparing to phase difference introduced by frequency change, the effect of the input power can be negligible.

TABLE 1. Phase Difference With Variouw Input Power @1310 nm (dBm)

Frequency (MHz)	Power Divider1			Fiber Splitter 1		
	0dBm	-3dBm	-5dBm	0dBm	-3dBm	-5dBm
100	-0.062	-0.122	-0.062	0.304	0.406	0.362
200	-0.043	-0.099	-0.312	0.983	1.034	1.020
300	-0.039	-0.098	-0.071	1.252	1.386	1.370
400	0.251	0.194	0.266	1.546	1.610	1.574
500	0.708	0.726	0.618	2.128	2.161	2.126
600	1.028	1.002	1.002	2.620	2.439	2.442
700	0.953	0.842	0.792	2.956	2.780	2.986
800	1.029	0.997	0.981	3.634	3.480	3.534
900	1.609	1.658	1.508	2.938	4.366	4.254
1000	1.8595	1.932	1.802	4.770	5.002	4.864
1100	1.779	1.922	1.866	5.410	5.538	5.424
1200	2.368	2.239	2.080	6.006	6.160	5.934
1300	2.378	2.372	2.484	6.724	7.050	6.649
1400	2.850	-3.759	2.756	7.478	7.712	7.280

The correlation of signal is decided by the phase difference (time delay) of time and frequency synchronization system, and the dependency curve is shown in Figure 10. We can see that the correlation coefficient decreases with the increase of phase difference. Signals among channels are positive (negative) corelated when the phase difference is smaller (larger) than 90°, and no relevance appears (correlation ecoefficiency of 0) when the phase difference is 90°. For instance, the transition time delay from positive to negative correlation gets to be 125 ps for an input signal of 2 GHz. The correlation of signals among antennas is the decisive factor of the imaging quality, and therefore, the phase difference should be as small as possible.

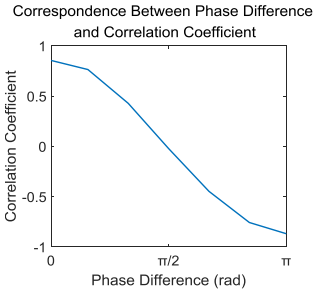

FIGURE 10. The correlation coefficients corresponding to the calculated phase differences of the signals.

According to the above tests, we can see that the phase difference between the output signals caused by fiber splitters can be eliminated by intercepting the optical fiber. And the phase difference between the output signals of power dividers is approximately in the same range of that of the fiber splitters in the entire testing frequency range. We should note that fiber splitters are more stable than power dividers. We also note that the power divider can only work in its limited working frequency range, while the fiber splitter can operate independent of the frequency of RF signal. To better realize the time alignment of signals in a heliograph, the optical splitters (after compensation) which provide smaller phase difference among channels could generate high-quality imaging of the Sun in most case. The tests for optical signal of both 1310nm and 1550 nm indicate that phase difference among channels could be eliminated by compensating the delay time introduced by the rear-end fiber of the optical splitters. Besides, we tested the effect of different powers on phase difference, and find the influence is negligible.

B. FREQUENCY STABILITY

The tests of the frequency stability were carried out in the thermostats in the temperature range of −10 °C to 30 °C and in the frequency range of 10MHz – 1GHz. The optical converter F-tone FTRFT-0PN55SF-U000 is used in the tests, and the wavelength of the optical signal is therefore 1550 nm. The frequency counter 53230A is utilized to calculate the Allan Variance. We note that the power divider 3 is tested in its working frequency range of 500 MHz ∼ 1 GHz. Results of the Allan variance at various frequency are recorded.

The frequency stability was first conducted for a relative short sampling time (100 ms). The short-term frequency stability mainly reflects the environmental impact on devices, and the jitters can lead to deterioration of the signal-to-noise ratio (SNR) of ADC, and thereby the data quality. The testing results are shown in Figure 11. As seen from this figure, at specific frequencies, the Allan Variances of fiber splitters (green, red and blue solid lines) decrease with the increasing temperature (ranging from −10 °C to 30 °C) for the entire testing frequency range. We note that this results from the microband effect, which leads to the signal loss and quality deterioration at low temperature [24]. On the other hand, the Allan Variances of the power dividers (black, orange and gray

dashed lines) get larger with increasing temperature at all frequencies. And this may be caused by the thermal noise which get worse with increasing temperature.

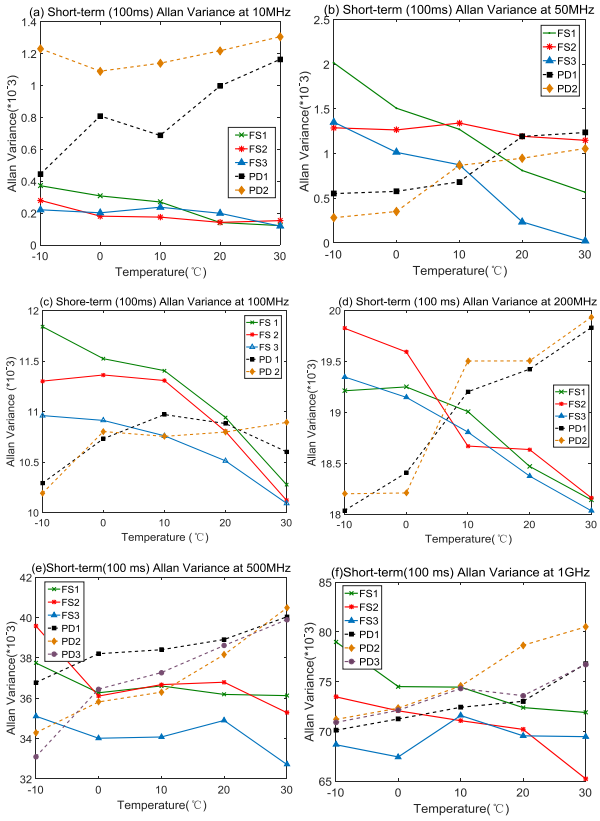

FIGURE 11. Dependence of short-term (100 ms) frequency stability (Allan Variance) for the three fiber splitters and the three power dividers on temperatures at 10 MHz (a), 50 MHz (b), 100 MHz (c), 200 MHz (d), 500 MHz (e) and 1.0 GHz (f). The results for fiber splitters are presented as the solid lines (green for FS1, red for FS2 and blue for FS3). The results for power dividers are presented as the dashed lines (black for PD1, orange for PD2 and gray for PD3). Because of the working frequency range of 500 MHz to 10 GHz for PD3, no results are shown in panel (a) – (d) for this device.

The frequency stability test was then conducted for a relative long sampling time (10 min). The long-term frequency stability reflects the stability of the clock, and the corresponding results are shown in Figure 12. We can see that the overall performance of the fiber splitters (solid lines) is better than those of the power dividers (dashed lines) at lower frequencies (≤200MHz) in the test. We should note that at higher frequency range (panel (c)-(f) in Figure 12), the difference of Allan Variance between fiber splitters and power dividers is quite small, and at some temperatures, say $< 0°$, the performance of the fiber splitters is even worse than that of power dividers. However, we can still conclude that the fiber splitters are overall more stable than the power dividers.

Besides, to evaluate the effect of frequency stability on the received signal form the Sun, we estimated the SNR of the receiver. The SNR can be estimated by

$$SNR_{Jitter}[\text{dBc}] = -20\log\left(2\pi \cdot f_{in} \cdot T_{Jitter}\right) \quad (3)$$

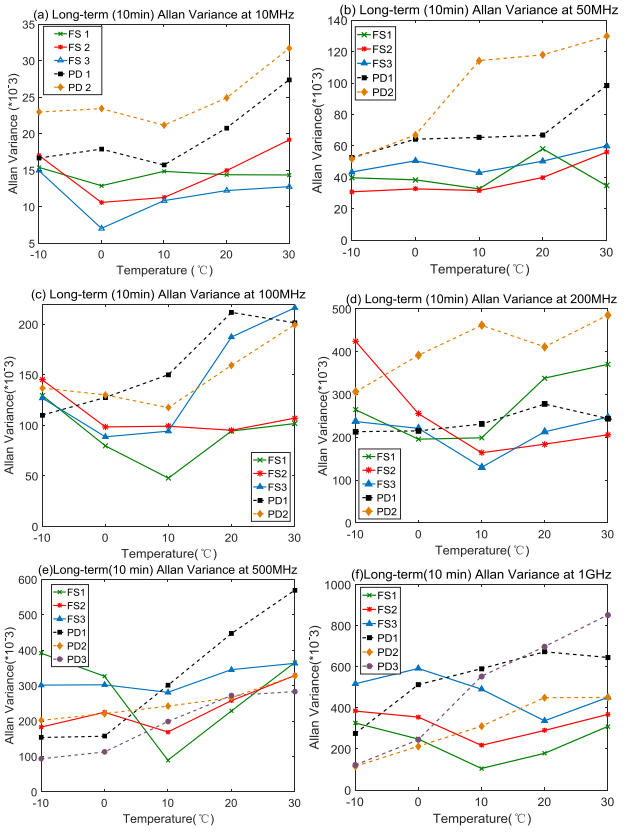

FIGURE 12. Dependence of long-term (10 min) frequency stability (Allan Variance) for the three fiber splitters and the three power dividers on temperatures at 10 MHz (a), 50 MHz (b), 100 MHz (c), 200 MHz (d), 500 MHz (e) and 1.0 GHz (f). The results for fiber splitters are presented as the solid lines (green for FS1, red for FS2 and blue for FS3). The results for power dividers are presented as the dashed lines (black for PD1, orange for PD2 and gray for PD3). Because of the working frequency range of 500 MHz to 10 GHz for PD3, no results are shown in panel (a) – (d) for this device.

TABLE 2. Estimated SNR of Power Divider 1 and Fiber Splitter 1.

Temperature (℃)	Power Divider1	Fiber Splitter 1
-10	46.579	46.459
0	46.579	46.617
10	46.505	46.691
20	46.478	46.502
30	46.245	46.429

where f_{in} is the frequency of the received signal, and T_{jitter} is the jitter of the sampling clock. The estimated SNRs of power divider 1 and fiber splitter 1 for solar emission at 2GHz are shown as Table 2. We can see that the SNR of ADC decreases slightly with the increasing temperature when using a power divider, while the SNR for the fiber splitter rises (falls) below (above) 10°C. This trend is the same as the Allan variance as shown in Figure 12. The difference between the signal splitting devices is not very significant, and a high sampling SNR and dynamic range can still be achieved using optical splitters.

According to the above tests, both fiber splitters and power dividers are sensitive to temperature. Fiber splitters have better short-term frequency stabilities at high temperature ($\geq$10°C), and power dividers have a better short-term frequency stability when working at the temperature below 10°C. As for long-term frequency stability, fiber splitters are more stable than the power dividers. To achieve the synchronization of time and frequency signals, it is necessary to compensate the error caused by environment change. Because the deterioration is determined by both temperature and frequency, we should decide which devices to use based on these two parameters. In our solution, at higher temperatures ($\geq$10°C), the fiber splitter is more suitable for transmitting standard frequency signals in order to obtain a higher SNR and dynamic range. At lower temperatures ($<$10°C), the performance of power divider is slightly better than fiber splitter.

IV. SUMMARY AND DISCUSSION

In the realization of a solar radio aperture synthesis system, the time signal (1PPS) and frequency signal should be divided and transmitted into all channels to realize the time and frequency synchronization. Time synchronization accuracy determines the correlation coefficient of the binary interferometer, which will affect the confidence of the heliograph imaging, and therefore the phase difference (time delay) between the timing signals is required to be as small as possible.

Fiber splitters and power dividers are widely used in RF signal splitting. However, the influence of them on the radio transmission has not been sufficiently studied. In this article, we conducted the study to find out the influence of the splitting devices on the phase difference of output signals between different channels and the deterioration of frequency stability.

The phase difference introduced by the fiber splitter's output is mainly caused by the length of the fiber at the rear end of the splitter, and it can be eliminated by compensating the length of the fibers. When excluding the influence from the fiber, we can find that the phase difference between different channels can be restricted in the range of $\sim \pm 1°$. On the other hand, the phase difference between the output signals of the power dividers has no discernible regularity with increasing frequency. The phase difference is not larger than $\pm 4°$ in the testing frequency range. Besides, we tested the effect of input powers on phase difference, and find the influence is negligible. According to the relationship between phase difference and correlation coefficient, we believe that when using fiber splitter, the imaging effect of heliograph could be much better.

Both short-term (100 ms) and long-term (10 min) frequency stability of both fiber splitter and power divider are tested in the frequency range of 10MHz $\sim$ 1GHz and in the temperature range of $-10°$C $\sim$ 30°C. In tests of short-term stability, the fiber splitters become more stable with increasing temperature while the performance of the power dividers get worse. In tests of long-term frequency stability, the fiber splitters performs better than power dividers at most frequencies for relatively low temperature ($\leq$10°C). We note that the difference between fiber splitters and power dividers is not significant, and the SNR introduced by an optical splitter could be slightly larger, which may result in a better performance of the heliograph.

These tests provide supports for the construction of a time and frequency synchronization system. The fiber splitter performs better in our tests and it may be a better choice in the design of a new time synchronization system. Firstly, the power dividers, though yield a phase difference of $\sim \pm 4°$, could only operate in its working frequency range, while the fiber splitter can split signals at various frequencies with even smaller phase difference. Secondly, the power divider can only split and transmit signals into a few channels, while the fiber splitter can easily divide signals into dozens or even hundreds of channels. Moreover, the fiber splitter is more stable than the power divider in our tests, and can provide a higher SNR. Therefore, the fiber splitter could be an appropriate option for multi-branch, wideband systems. Besides, the adoption of fiber splitter can save a large amount of cost in optical transmitter. We should also note that when adopting a Round-Trip time-frequency synchronization system with fiber splitters, other equipment, such as optical circulator, may be introduced. And those devices may result in a final cost that may be no less than using a power divider. The results can support the selection of devices in the heliograph to obtain better observation results, and provide a feasible solution of the construction of low-cost radioheliograph.

The tests in this article are mainly designed for the time and frequency synchronization system for radioheliograph. Because of the limitation of testing instruments, the tests were carried out for the phase difference tests in a limited frequency range of 10 MHz to 1.4 GHz, the frequency stability in the frequency range of 10 MHz $-$ 1GHz in the temperature range of -10 °C $-$ 30 °C. A larger frequency range needs to be considered in subsequent studies.

REFERENCES

[1] H. N. Bhalme and D. A. Mooley, "Cyclic fluctuations in the flood area and relationship with the double (Hale) sunspot cycle," *J. Appl. Meteorol.*, vol. 20, no. 9, pp. 1041–1048, Sep. 1981.

[2] K. O'Brien, W. Friedberg, H. H. Sauer, and D. F. Smart, "Atmospheric cosmic rays and solar energetic particles at aircraft altitudes," *Environ. Int.*, vol. 22, pp. 9–44, Jan. 1996.

[3] W. S. Kurth, "The great solar storms of 1989," *Nature*, vol. 353, no. 6346, pp. 705–706, Oct. 1991.

[4] S. Song, N. Cheng, H. Xie, and W. Zhou, "Adaptability of GPS/BDS broadcast ionospheric models to solar activities," *Adv. Space Res.*, vol. 63, no. 9, pp. 2867–2876, May 2019.

[5] R. J. Redmon, D. B. Seaton, R. Steenburgh, J. He, and J. V. Rodriguez, "September 2017's geoeffective space weather and impacts to caribbean radio communications during hurricane response," *Space Weather*, vol. 16, no. 9, pp. 1190–1201, Sep. 2018.

[6] A. R. Thompson and J. Moran, "Introductory theory of interferometry and synthesis imaging," in *Interferometry and Synthesis in Radio Astronomy*, 3rd ed. Gewerbestrasse, Switzerland: Springer, 2017, ch. 2, sec. 1–3, pp. 59–74.

[7] V. M. Nakariakov, L. K. Kashapova, and Y.-H. Yan, "Editorial: Solar radiophysics—Recent results on observations and theories," *Res. Astron. Astrophys.*, vol. 14, no. 7, pp. E1–E6, Jul. 2014.

[8] Y. Chen, S. Feng, F. Yan, C. Chen, Y. Su, R. Cheng, J. Zhang, Q. Du, and X. Li, "A compensation method for the consistency of multi-channel mixing circuit for solar radio observation system," *Scientia Sinica Technologica*, vol. 49, no. 8, pp. 901–909, Aug. 2019.
[9] F. Yan, J. Liu, Y. Su, X. Zheng, G, Zhao, "A study on uncertainty and error of sampling clock in electromagnetic prospecting system," *Chin J. Geophys.*, vol. 60, no. 11, pp. 4204–4211, Nov. 2017.
[10] F. Yan, Y. Liu, K. Xu, Z. Shang, Y. Su, G. Lu, Y. Chen, and W. Zhao, "A broadband digital receiving system with large dynamic range for solar radio observation," *Res Astron Astrophys*, vol. 20, no. 9, pp. 159–164, Sep. 2020.
[11] K. Xu, Z. Shang, F. Yan, Y. Liu, Z. Wu, Y. Zhang, L. Zhang, Y. Su, and Y. Chen, "Study on the compensation method of signal flatness for a broadband solar millimeter radio observation system," *Sci. Sinica Tech.*, to be published. [Online]. Available: https://engine.scichina.com/publisher/scp/journal/SST/doi/10.1360/SST-2020-0283?slug=fulltext, doi: 10.1360/SST-2020-0283.
[12] H. Nakajima, M. Nishio, S. Enome, K. Shibasaki, T. Takano, Y. Hanaoka, C. Torii, H. Sekiguchi, T. Bushimata, S. Kawashima, N. Shinohara, Y. Irimajiri, H. Koshiishi, T. Kosugi, Y. Shiomi, M. Sawa, and K. Kai, "The nobeyama radioheliograph," *Proc. IEEE*, vol. 82, no. 5, pp. 705–713, May 1994.
[13] V. Grechnev, V. Lesovoi, G. Smolkov, B. Krissinel, V. Zandanov, A. Altyntsev, N. Kardapolova, R. Sergeev, A. Uralov, V. Maksimov, and B. Lubyshev, "The siberian solar radio telescope: The current state of the instrument, observations, and data," *Sol. Phys.*, vol. 216, no. 1, pp. 239–272, Jan. 2003.
[14] X. Deng, J. Liu, D. Jiao, J. Gao, Q. Zhang, G. Xu, R. Dong, T. Liu, and S. Zhang, "Coherent transfer of optical frequency over 112 km with instability at the 10 (-20) level," *Chin. Phys. Lett.*, vol. 33, no. 11, pp. 51–53, Nov. 2016.
[15] S. W. Schediwy, D. R. Gozzard, C. Gravestock, S. Stobie, R. Whitaker, J. A. Malan, P. Boven, and K. Grainge, "The mid-frequency square kilometre array phase synchronisation system," *Publications Astronomical Soc. Aust.*, vol. 36, p. 7, Feb. 2019.
[16] D. Gozzard, S. Schediwy, R. Dodson, M. Rioja, M. Hill, B. Lennon, J. McFee, P. Mirtschin, J. Stevens, and K. Grainge, "Astronomical verification of a stabilized frequency reference transfer system for the square kilometer array," *Astronomical J.*, vol. 154, no. 1, pp. 154–162, Jul. 2017.
[17] B. Wang, X. Zhu, C. Gao, Y. Bai, J. W. Dong, and L. J. Wang, "Square kilometre array telescope—Precision reference frequency synchronisation via 1f-2f dissemination," *Sci. Rep.*, vol. 5, no. 1, pp. 66–75, Sep. 2015.
[18] X. Dan, W. Lee, F. Stefani, O. Lopez, A. Amy-Klein, and P. Pottie, "Studying the fundamental limit of optical fiber links to the 10^{21} level," *Opt. Exp.*, vol. 26, no. 8, pp. 9515–9527, Apr. 2018.
[19] Q. Liu, W. Chen, D. Xu, N. Cheng, F. Yang, Y. Gui, H. Cai, and S. Han, "Simultaneous frequency transfer and time synchronization over a cascaded fiber link of 230 km," *Chin J Las.*, vol. 43, no. 3, Mar. 2016, Art. no. 0305006.
[20] L. Wang, G. Wu, J. Shen, L. Hu, and J. Chen, "Simultaneous transfer of time and frequency over 100 km fiber link," *Acta Optica Sinica*, vol. 35, no. 4, 2015, Art. no. 0406004.
[21] X. Zhu, B. Wang, C. Gao, J. Dong, and L. Wang, "Application of ultra-stable frequency synchronization in the square kilometer array," *Act Meterologica Sinica*, vol. 36, no. 6A, pp. 116–119, Dec. 2015.
[22] Y. Yuan, B. Wang, and L. Wang, "Fiber-based joint time and frequency dissemination via star-shaped commercial telecommunication network," *Chin. Phys. B.*, vol. 26, no. 8, pp. 100–105, Aug. 2017.
[23] K. Turza, P. Krehlik, and L. Sliwczynski, "Long haul time and frequency distribution in different DWDM systems," *IEEE Trans. Ultrason., Ferroelectr., Freq. Control*, vol. 65, no. 7, pp. 1287–1293, Jul. 2018.
[24] M. Huo, "Influence of packaging technology of optical splitter on optical signal loss in severe cold area," *Cable Telev. Tech.*, vol. 9, no. 1, pp. 122–130, Sep. 2008.

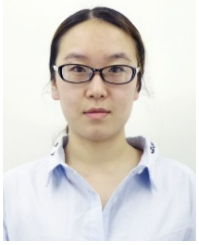

YUQING LIU was born in Jinan, Shandong, China, in 1997. She received the B.S. degree in measurement-control technology and instrumentation from the Harbin Institute of Technology, in 2018. She is currently pursuing the degree in geophysics with Shandong University.

Her research interests include solar radio telescope systems, and fiber-based time and frequency synchronization.

DAOPENG REN was born in Zibo, Shandong, China, in 1996. He received the B.S. degree in measurement-control technology and instrumentation from Shandong University, in 2019, where he is currently pursuing the master's degree in geophysics.

His research interests include time-frequency synchronization in radio and high-precision data acquisition.

FABAO YAN was born in Xiangyang, Hubei, China, in 1985. He received the B.S. degree in measurement-control technology and instrumentation from the Harbin Institute of Technology, in 2008, the M.S. degree in computer application technology from the Chinese Academy of Mechanical Sciences, in 2011, and the Ph.D. degree in geodetection and information technology from Central South University, Changsha, Hunan, in 2016. From 2008 to 2011, he was a Research Assistant with the Southwest Automation Institute. Since 2012, he has been an Engineer with the Southwest Automation Institute. He was an Associate Professor of the Laboratory for ElectromAgnetic Detection, Institute of Space Sciences, Shandong University, where he is currently the Director and a CTO. He has authored one book, more than 20 articles, and more than 20 inventions. His research interests include solar radio telescope systems and precision instruments.

ZHAO WU received the B.S. degree in applied physics from Shandong University, Weihai, China, in 2007, and the M.S. and Ph.D. degrees in theoretical physics from Shandong University, in 2010 and 2019, respectively.

Since 2010, he has been a Lecturer with the School of Space Science and Physics, Shandong University, China. His research interests include the observation of microwave bursts during solar eruption and the development of corresponding digital receiver.

ZHEN DONG was born in Zibo, Shandong, China, in 1997. He received the B.S. degree in electronic and information engineering from the China University of Petroleum, in 2019. He is currently pursuing the master's degree in electronics and communication engineering with Shandong University.

His research interests include solar radio digital receiver and digital correlator.

YAO CHEN received the B.S. and Ph.D. degrees in solar-terrestrial space physics from the University of Science and Technology of China, in 1997 and 2004, respectively.

He is currently a Distinguished Professor of Shandong University, where he is also the Executive Director of the Institute of Space Science. He has published more than 100 SCI articles, which have been cited for thousands of times. His research interests include heating and accelerating mechanism of corona and solar wind, solar eruption, such as mass ejection dynamics of corona, fluctuation in space plasma, and the related application of space weather. He was the winner of the National Science Fund for Distinguished Young Scholars.